

Search for radiative $\Upsilon(1S)$ decays into light mesons

Crystal Ball Collaboration

P. Schmitt^{1,2}, D. Antreasyan⁸, H.W. Bartels⁴, D. Besset¹⁰, Ch. Bieler⁷, J.K. Bienlein⁴, A. Bizzeti⁶, E.D. Bloom¹¹, I. Brock², K. Brockmüller⁴, R. Cabenda¹⁰, A. Cartacci⁶, M. Cavalli-Sforza^{10,a}, R. Clare¹¹, A. Compagnucci⁶, G. Conforto⁶, S. Cooper^{11,b}, R. Cowan¹⁰, D. Coyne^{10,a}, A. Engler², K. Fairfield¹¹, G. Folger⁵, A. Fridman^{11,c}, J. Gaiser¹¹, D. Gelpman¹¹, G. Glaser⁵, G. Godfrey¹¹, F.H. Heimlich⁷, R. Hofstadter¹¹, J. Irion⁸, Z. Jakubowski³, K. Karch¹², S. Keh¹², H. Kilian¹², I. Kirkbride¹¹, T. Kloiber⁴, M. Kobel⁵, W. Koch⁴, A.C. König⁹, K. Königsmann^{12,d}, R.W. Kraemer², S. Krüger⁷, G. Landi⁶, R. Lee¹¹, S. Leffler¹¹, R. Lekebusch⁷, W. Lockman¹¹, S. Lowe¹¹, B. Lurz⁵, D. Marlow², H. Marsiske⁴, W. Maschmann⁷, P. McBride⁸, H. Meyer⁴, B. Muryn³, F. Messing², W.J. Metzger⁹, B. Monteleoni⁶, R. Nernst⁷, B. Niczyporuk¹¹, G. Nowak³, C. Peck¹, P.G. Pelfer⁶, B. Pollock¹¹, F.C. Porter¹, D. Prindle², P. Ratoff¹, M. Reidenbach⁹, B. Renger², C. Rippich², M. Scheer¹², J. Schotanus⁹, J. Schütte⁵, A. Schwarz¹¹, D. Sievers⁷, T. Skwarnicki⁴, V. Stock⁷, K. Strauch⁸, U. Strohbusch⁷, J. Tompkins¹¹, H.J. Trost⁴, B. van Uiter¹¹, R.T. Van de Walle⁹, H. Vogel², A. Voigt⁴, U. Volland⁵, K. Wachs⁴, K. Wacker¹¹, W. Walk⁹, H. Wegener⁵, D. Williams⁸, P. Zschorsch⁴

¹ California Institute of Technology, Pasadena, CA 91125, USA

² Carnegie-Mellon University, Pittsburgh, PA 15213, USA

³ Cracow Institute of Nuclear Physics, PL-30055 Cracow, Poland

⁴ Deutsches Elektronen Synchrotron DESY, D-2000 Hamburg, Federal Republic of Germany

⁵ Universität Erlangen-Nürnberg, D-8520 Erlangen, Federal Republic of Germany

⁶ INFN and University of Firenze, I-50100 Firenze, Italy

⁷ Universität Hamburg, I. Institut für Experimentalphysik, D-2000 Hamburg, Federal Republic of Germany

⁸ Harvard University, Cambridge, MA 02138, USA

⁹ University of Nijmegen and NIKHEF, NL-6525 ED Nijmegen, The Netherlands

¹⁰ Princeton University, Princeton, NJ 08544, USA

¹¹ Department of Physics, HEPL, and Stanford Linear Accelerator Center, Stanford University, Stanford, CA 94305, USA

¹² Universität Würzburg, D-8700 Würzburg, Federal Republic of Germany

Received 21 March 1988; in revised form 30 May 1988

Abstract. We have searched for radiative decays of the $\Upsilon(1S)$ resonance, $\Upsilon(1S) \rightarrow \gamma X$, where X is one of the mesons $\eta, \eta', f_2(1270), f_2(1720)$, or a narrow resonance with mass less than $3 \text{ GeV}/c^2$ which decays into either $\pi^0 \pi^0$ or $\eta \eta$. The mesons are identified in their all-neutral decay modes. Since we do not find any such decays, we calculate upper limits on the corresponding branching ratios. These limits are compared to theoretical predictions and to the corre-

sponding branching ratios measured in radiative J/ψ decays.

Introduction

The main decay modes of a heavy narrow vector meson like the $\Upsilon(1S)$ result from the annihilation of its constituents, a heavy quark and antiquark. The decay mode with the largest rate is described in lowest order QCD by a three gluon intermediate state which fragments with probability one into hadrons. Another important decay mode proceeds similarly except that one of the gluons is replaced by a photon [1]. The two gluons hadronize into ordinary mesons or they may form gluonium states, which consist in lowest

Present addresses:

^a Inst. for Particle Physics, University of California, Santa Cruz, CA 95064, USA

^b Massachusetts Institute of Technology, Cambridge, MA 02139, USA

^c DPHPE, Centre d'Etudes Nucléaires de Saclay, F-91191 Gif sur Yvette, France

^d Sektion Physik, Universität München, D-8000 München, FRG

order of two gluons. Therefore the study of radiative decays of heavy bound $Q\bar{Q}$ states may provide insight into the formation mechanism and the gluonic content of light mesons. Radiative decays of the J/ψ have been measured [2] with branching ratios of the order of 10^{-3} and have revealed two gluonium candidate states [3, 4], the $\eta(1440)$ and $f_2(1720)$. Thus it is of considerable interest to also search for radiative decays of the $\Upsilon(1S)$ resonance to these gluonium candidates and to other light mesons.

Radiative decay rates can be calculated [5–7] within the framework of QCD. The coupling of gluons to heavy quarks can be treated perturbatively, whereas the coupling of gluons to light quarks has to be determined with low-energy non-perturbative matrix elements. By forming ratios of decay rates for different quarkonia states, the uncertain matrix elements cancel and the ratios will depend on quark masses m_Q only. In particular, the $\Upsilon(1S)$ radiative branching ratio $B(Y \rightarrow \gamma X)$ is found in most theoretical calculations [5, 6, 7] to be suppressed by about $(e_b/e_c)^2 (m_c/m_b)^2 \simeq 1/40$ with respect to the J/ψ branching ratio $B(J/\psi \rightarrow \gamma X)$, where e_Q is the charge and m_Q the mass of the quark. Therefore, rather large data samples are needed to study radiative $\Upsilon(1S)$ decays.

Data sample and detector

The analysis presented here is based on 46 pb^{-1} of data collected on the $\Upsilon(1S)$ resonance, corresponding to $(476 \pm 20) \times 10^3$ produced $\Upsilon(1S)$ mesons. A second data sample of 20 pb^{-1} on the $\Upsilon(4S)$ resonance was used for background studies. The data were collected with the Crystal Ball detector at the e^+e^- storage ring DORIS II at DESY. Photon energies and directions are measured in the main part of the detector, a spherical shell of 672 NaI(Tl) crystals covering 93% of 4π . For electromagnetically showering particles the energy resolution is given by $\sigma_E/E = (2.7 \pm 0.2)\% / \sqrt[4]{E/\text{GeV}}$, and the polar angular resolution is $\sigma_\theta = 2^\circ$ to 3° , slightly depending on energy. Photons, electrons and positrons yield a rather symmetric lateral energy deposition pattern with typically 70% of the energy deposited in one crystal and about 98% in 13 contiguous crystals. Proportional tube chambers surrounding the beam pipe detect charged particles. A more detailed description of the detector can be found in reference [8].

Because of its good photon energy resolution, the Crystal Ball detector is well suited to search for radiative decays of the $\Upsilon(1S)$ resonance to mesons which decay with large branching fractions into all-neutral final states. In particular those final states are used which contain π^0 's [$B(\pi^0 \rightarrow \gamma\gamma) = 98.8\%$] and η 's

[$B(\eta \rightarrow \gamma\gamma) = 39\%$ and $B(\eta \rightarrow 3\pi^0) = 32\%$ [2]]. The following decay models, all measured on the J/ψ with a substantial branching ratio, were searched for on the $\Upsilon(1S)$:

$$\begin{aligned} \Upsilon(1S) &\rightarrow \gamma\eta \\ \Upsilon(1S) &\rightarrow \gamma\eta', \quad \eta' \rightarrow \eta\pi^0\pi^0 \\ \Upsilon(1S) &\rightarrow \gamma f_2(1270), \quad f_2(1270) \rightarrow \pi^0\pi^0 \\ \Upsilon(1S) &\rightarrow \gamma f_2(1720), \quad f_2(1720) \rightarrow \eta\eta. \end{aligned} \quad (1)$$

The $f_2(1720)$ resonance, a strong gluonium candidate, was originally discovered [4] in the channel $\eta\eta$. Therefore we have extended our search for other narrow resonances X with width $\Gamma_X < 50 \text{ MeV}$ and mass less than $3 \text{ GeV}/c^2$ in the decay chains:

$$\begin{aligned} \Upsilon(1S) &\rightarrow \gamma X, \quad X \rightarrow \pi^0\pi^0 \\ \Upsilon(1S) &\rightarrow \gamma X, \quad X \rightarrow \eta\eta. \end{aligned} \quad (2)$$

The advantage of a search for $\pi^0\pi^0$ over $\pi^+\pi^-$ arises from the fact that iso-vector resonances do not decay into the former channel. Thus a possible feed-down from $\Upsilon(1S)$ decays to $\pi^0\rho^0$, $\pi^0\rho^0(1600)$ and $\pi^0\rho_3^0(1690)$ will be absent.

If the meson X produced in radiative decays has a mass small compared to the $\Upsilon(1S)$ mass M_Y , its Lorentz boost is given by $E_X/m_X \simeq M_Y/2m_X \gg 1$. Due to this rather large boost all the meson decay products tend to cluster in a narrow cone opposite to the radiative photon. Even with the finely segmented Crystal Ball detector it is not possible to disentangle the energies and impact points of all the individual photons from the decay of the meson. However, the invariant mass of the photons and thus the mass of the decaying meson can be reconstructed to good approximation. This is achieved with the ‘‘global shower technique’’ [9], by which the invariant mass of a shower is estimated from the second moment of the energy deposition. This will be described in detail in the next section.

Another algorithm called ‘‘PIFIT’’ [9] is used which performs maximum likelihood fits to the pattern of energy deposition using the hypotheses that either two photons or one photon created the shower, respectively. For an energy deposition of multi-photon origin the two-photon hypothesis will also be very likely. Thus the difference in the log-likelihood [10] of the two hypothesis is used as a quantitative measure whether a shower is more consistent with multi-photon or one-photon origin.

For the particular decay mode $\Upsilon(1S) \rightarrow \gamma\eta$, $\eta \rightarrow 2\gamma$ one energy cluster is due to exactly two photons. In this case the difference in the log-likelihood from PIFIT alone can be used to discriminate between show-

ers arising from a single photon and from two photons. For overlapping showers originating from two photons PIFIT yields in addition an estimate on the impact point of the two photons, thus allowing the reconstruction of an invariant mass. The analysis for this specific channel involving the PIFIT algorithm alone will be presented in a later section.

Global shower analysis

The global shower technique uses an energy cluster, defined as a contiguous region of crystals where each crystal has more than 10 MeV of deposited energy E_i . The total energy in the cluster is given by $E = \sum_i E_i$, where the sum extends over all crystals in the cluster. The direction of the center of gravity of each energy cluster is defined by $\mathbf{c} = \frac{1}{E} \sum_i \hat{c}_i E_i$ where \hat{c}_i is the unit vector pointing to the center of the i^{th} crystal. The second moment of the cluster is calculated with $S = \frac{1}{E} \sum_i (\mathbf{c} - \hat{c}_i)^2 E_i$. The invariant mass M of the cluster is then obtained from the relation $M = f E \sqrt{S - S_y}$, where $S_y = 4.0 \times 10^{-3} \text{ rad}^2$ is a measure of the average width of a single photon cluster. The non-vanishing value of S_y arises mainly from the granularity of the detector and is determined with Monte Carlo meth-

ods based on the electron gamma shower program EGS [11]. The function f absorbs the contribution from higher orders in M/E . Over the mass range investigated it was found to be constant to a good approximation, $f = 1.08$. If the decay products of a meson form more than one energy cluster, each cluster is assigned an invariant mass, an energy, and a direction and thus a four-vector. These four-vectors are then combined to obtain the invariant mass of the decaying meson.

Figure 1a illustrates the result of such an analysis for Monte Carlo events [12] of the type $Y(1S) \rightarrow \gamma \eta'$, $\eta' \rightarrow \eta \pi^0 \pi^0$, $\eta \rightarrow 3\pi^0$. The solid histogram represents the mass distribution for the radiative photon. The depletion of events at low masses is due to the Jacobi transformation from the second moment to the invariant mass. The η' decay products forming one energy cluster yield the mass distribution shown as the dashed histogram. It is consistent with a Gaussian positioned at 960 MeV/ c^2 and with a width of 60 MeV. Figure 1b shows the difference in PIFIT log-likelihood, $\Delta \mathcal{L}$, for the two-photon and one-photon hypotheses for the same Monte Carlo events. A bin size of 0.1 was chosen for the solid histogram from the radiative photon. The dashed histogram representing the energy cluster from the η' however is shown with a larger bin size of 1.0. Little overlap exists between single-photon and multi-photon clusters. In this case a cut of $\Delta \mathcal{L} > 2.5$ will retain 86% of the multi-photon clusters.

The Monte Carlo events for Y radiative decay into the pseudoscalars η and η' were generated with a photon angular distribution of $1 + \cos^2 \theta_\gamma$, where θ_γ is the angle of the photon with respect to the beam direction. The angular distributions of the subsequent decays $\eta \rightarrow 3\pi^0$ and $\eta' \rightarrow \eta \pi^0 \pi^0$ were generated isotropically since no evidence has been found [13, 14] for deviations from phase space. As the helicity structure for $Y(1S)$ radiative decays to spin 2 mesons is unknown, we chose isotropic distributions for the production and decays of $f_2(1270)$ and $f_2(1720)$. The X states were also generated isotropically and with zero intrinsic width. Finally, the interaction of the final state photons in the detector was simulated using the electron gamma shower program EGS [11].

The event selection criteria to be described in the following section were then applied to the Monte Carlo events. For mesons with a narrow width (η , η' , X) fits to the Monte Carlo invariant mass spectra yield Gaussian line shapes positioned within ± 10 MeV/ c^2 of the nominal meson masses. The widths of the Gaussians were found to be independent of the number of energy clusters produced by the meson. However, the width increases with increasing meson mass and ranges from 50 MeV for low mass mesons to 90 MeV

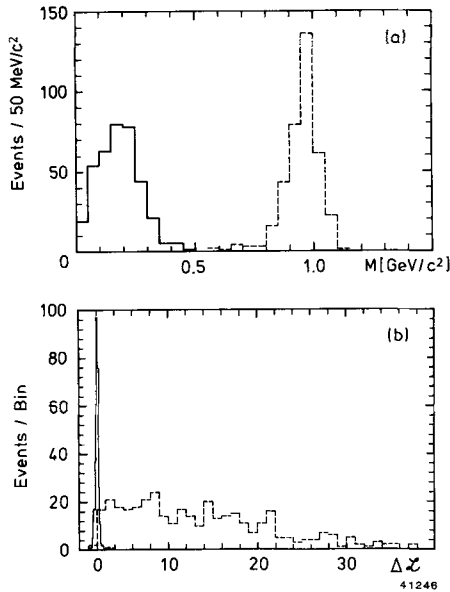


Fig. 1a, b. Distributions of the shower mass **a** and the difference in log-likelihood **b** for Monte Carlo events of the type $Y(1S) \rightarrow \gamma \eta'$, $\eta' \rightarrow \eta \pi^0 \pi^0$, $\eta \rightarrow 3\pi^0$. The solid histograms are the distributions from the radiative photon, whereas the dashed histograms are from single energy clusters originating from the decay products of the η' . The bin size in **b** is 0.1 and 1.0 for the photon and η' histograms respectively

for high mass mesons. Due to the larger natural widths [12] of the $f_2(1270)$ and $f_2(1720)$ mesons, the Monte Carlo mass resolutions also turn out to be larger: 127 MeV and 144 MeV, respectively, but consistent with Gaussian shapes.

Event selection

We are looking for events of the type $\Upsilon(1S) \rightarrow \gamma X \rightarrow n\gamma$ with all of the energy deposited in the detector. Events are selected with at least 8.5 GeV of total detected energy, and having two, three or four energy clusters. The neutrality of each cluster is ascertained by the requirement that there is no correlated track in the proportional chambers. For each energy cluster in the event we calculate \mathbf{c} and M . The total momentum of all clusters is then given by $\mathbf{p} = \sum_j \mathbf{c}_j E_j$, where E_j is the energy of the j^{th} cluster with direction \mathbf{c}_j defined as above. To ensure approximate momentum balance we require the transverse momentum $|p_t| < 1.5$ GeV/c and the longitudinal momentum $|p_z| < 2.0$ GeV/c. The larger cut for p_z takes into account the width $\sigma_z = 1.2$ cm of the distribution of the production vertex, which cannot be corrected for event-by-event. For events with exactly two clusters we require at least one cluster with an invariant mass larger than 200 MeV.

The definition of the radiative photon candidate is straightforward. For events with two energy clusters, the photon candidate is the cluster with the lower invariant mass. For events with three or four energy clusters, the photon candidate is the cluster most isolated in space. To reduce background, we require the photon candidate to be within $|\cos \theta_\gamma| < 0.8$. Background arises mainly from (radiative) QED events $e^+ e^- \rightarrow \gamma\gamma(\gamma)$ and $e^+ e^- \rightarrow e^+ e^- (\gamma)$, where in the latter case both, the final state electron and positron, are not detected by the proportional chambers due to inefficiency. Both processes are peaked towards the beam direction. Background from hadronic events is very small due to the multiplicity cut of less than four clusters.

We now turn to the analysis of those clusters originating from the meson decay products opposite to the photon candidate. Mesons produced in the radiative decay of the $\Upsilon(1S)$ get a Lorentz boost inversely proportional to their mass. Thus the decay products of light mesons tend to produce fewer energy clusters in the detector than do heavier mesons. To maximize the signal-to-noise ratio we group the events according to the number of clusters produced and analyze the two groups with somewhat different cuts. Light mesons are sought in events containing two or three neutral energy clusters (2–3), i.e. one or two clusters

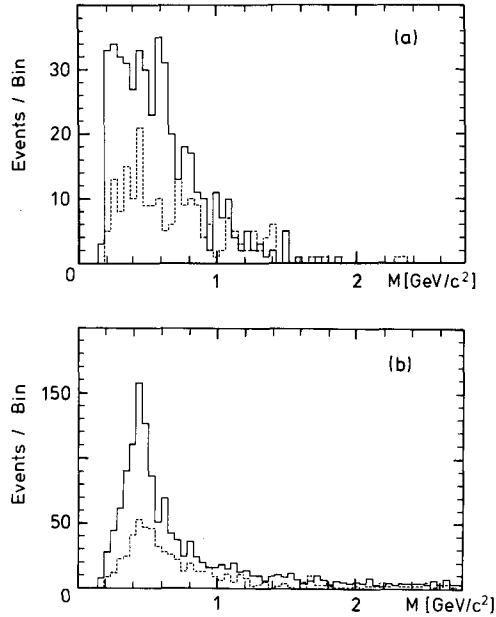


Fig. 2 a, b. Spectra of invariant masses recoiling against the radiative photon for data collected on the $\Upsilon(1S)$ resonance (solid histogram) and on the $\Upsilon(4S)$ (dashed histogram). **a** shows the result from the data set with two and three energy clusters (2–3), **b** with three and four energy clusters (3–4). The bin size is 54 MeV

from the meson decay plus an additional cluster from the radiative photon. Events containing three or four clusters (3–4) are used to search for heavier mesons. In the intermediate mass region, around 1.5 to 2 GeV/c^2 , both analyses yield consistent results. In the following we refer to the two analyses by the cluster content, (2–3) or (3–4), respectively.

To ensure that at least one cluster opposite to the photon candidate indeed originates from overlapping photons, a maximum likelihood fit using PIFIT is performed to test the hypothesis of many photon vs. one photon origin. For events with two energy clusters the meson candidate is required to have a log-likelihood difference $\Delta\mathcal{L}$ for the two-photon and one-photon hypotheses [10] of larger than 2.5. Three cluster events are treated differently for the (2–3) and (3–4) cluster analyses. The (2–3) analysis requires the highest of the two energy clusters from the meson decay to have $\Delta\mathcal{L} > 2.5$. In the high mass (3–4) analysis however, the highest energy cluster is often due to a single photon from the meson decay fragments. Therefore we require the second highest energy cluster to satisfy $\Delta\mathcal{L} > 1.5$. No constraint is necessary for the four cluster topology because of smaller background. The resulting data sample consists of 458 events for the (2–3) analysis. Due to softer cuts, 1314 events pass the (3–4) analysis.

The invariant mass of the meson candidates is plotted for the (2–3) and (3–4) analyses in Fig. 2a, b as the solid histogram. The magnitude of the spectrum in Fig. 2a is dominated by the two cluster subsample. Broad clusters from shower fluctuations and overlapping photons cause the enhancement at low invariant mass. The sharp rise at 200 MeV originates from the invariant mass cut for two cluster events. The (3–4) spectrum, Fig. 2b, shows a peak around 400 MeV, which is due to configurations of clusters located closely in space. These arise from radiative QED events with shower fluctuations in the detector.

To verify that the distributions are compatible with background from QED and hadronic events, we performed the same analysis on 20 pb^{-1} of data accumulated on the $\Upsilon(4S)$ resonance. The $\Upsilon(4S)$ state decays dominantly into pairs of B -mesons. Radiative decays are suppressed by the ratio of total widths [2] $\Gamma_{\text{tot}}(\Upsilon(1S))/\Gamma_{\text{tot}}(\Upsilon(4S)) \simeq 2 \times 10^{-3}$ and are thus unobservable with our present sensitivity. The mass spectra obtained from this data sample are shown in Fig. 2 for both analyses as the dashed histograms. Fitting the shape of the $\Upsilon(1S)$ data to that of the $\Upsilon(4S)$ data yields a χ^2 of 67 and 86 for 59 degrees of freedom for the (2–3) and (3–4) cluster data sets, respectively, and normalization factors of 0.43 ± 0.03 (2–3) and 0.43 ± 0.02 (3–4). We expect that the background arises mainly from QED processes. Therefore these values should be in agreement with the ratio of luminosities times cross section, where the cross section scales with inverse mass squared of the Υ mesons: $(L_{4S}/L_{1S}) \times (M_{1S}^2/M_{4S}^2) = (20/46) \times (9.46/10.577)^2 = 0.35$. The discrepancy between data and expectation reflects the varying performance of the proportional chambers. A small change in detection inefficiency for charged particles results in substantial additional background from the large Bhabha scattering cross section. Therefore we do not subtract the normalized spectra but rather use the uncorrected $\Upsilon(1S)$ spectra for further analysis.

Both invariant mass spectra from $\Upsilon(1S)$ data in Fig. 2 show no structure consistent with our experimental resolution. To obtain upper limits we fitted the spectra with Gaussians of fixed mass and width as determined from the Monte Carlo events. Legendre polynomials up to third order were used to accommodate the background shape. The mass interval fitted was at least $1 \text{ GeV}/c^2$ wide, corresponding to more than 12 standard deviations of our resolution. No signals with more than two standard deviations were found. For each individual fit, the 90% confidence level (CL) upper limit on the observed number of events was obtained by integrating the likelihood function up to 90% of its total area between $N=0$ and infinity. As an example, at the position of the

η' the fit yields an amplitude of $N = 5.5 \pm 8.3$ events, corresponding to a 90% CL upper limit of $N_{90\%} = 17.5$ events.

Efficiency determination

The efficiency ε_{MC} for all selection cuts except the requirement of neutrality was determined with the Monte Carlo generated events. Efficiencies of about 40% were found for radiative decays into η , η' and for low mass states X decaying into $\pi^0\pi^0$. With increasing $\pi^0\pi^0$ invariant mass the (2–3) cluster analysis becomes less efficient; above $1.5 \text{ GeV}/c^2$ we therefore use the (3–4) cluster analysis with an efficiency of 30%, nearly independent of mass. The efficiency for the $\gamma\eta\eta$ final state using the (2–3) cluster analysis decreases from 30% to 15% between threshold and $2.2 \text{ GeV}/c^2$; at this mass the (3–4) cluster analysis takes over with a constant efficiency of 15%.

The probability for events to pass the neutrality requirement was studied using the very clean two-photon process $e^+e^- \rightarrow e^+e^- f_2(1270), f_2 \rightarrow \pi^0\pi^0 \rightarrow 4\gamma$ and the QED processes $e^+e^- \rightarrow e^+e^-$ and $e^+e^- \rightarrow 2\gamma$. The weighted average of both methods yields an efficiency of $\varepsilon_\gamma = (93.3 \pm 1.5)\%$ for the detection of a photon as a neutral energy cluster. The error arises from the quadratic addition of statistical and systematic uncertainties. This neutral probability *per photon* includes the effects of photon conversion in the beam pipe or chambers and from accidental tagging due to random chamber hits. The neutral efficiency *per event* is then given by $\varepsilon_{ev} = \varepsilon_\gamma^n$ where n is the total number of photons for the event. As we analyzed two decay modes of the $\eta, \eta \rightarrow \gamma\gamma$ and $\eta \rightarrow 3\pi^0$, the final efficiency $\varepsilon_{\text{neut}}$ for a particular $\Upsilon(1S)$ decay to survive the cluster neutrality requirement, is the branching ratio times acceptance weighted average of ε_{ev} . For radiative decays into π^0 's only, $\varepsilon_{\text{neut}}$ is identical to ε_{ev} .

Results

With the number of produced $\Upsilon(1S)$ events, $N_\Upsilon = (476 \pm 20) \times 10^3$, the selection efficiency ε_{MC} , the neutral efficiency $\varepsilon_{\text{neut}}$, and the 90% CL upper limit $N_{90\%}$ on the observed number of events we calculate the 90% confidence level upper limit on the branching ratio with the formula

$$B < \frac{N_{90\%} \times (1 + 1.28 \sigma_{\text{rel}})}{\varepsilon_{MC} \varepsilon_{\text{neut}} N_\Upsilon}. \quad (3)$$

σ_{rel} is the quadratically combined fractional error of the efficiencies, the number of $\Upsilon(1S)$ decays and the errors on the measured branching ratios [2] of the

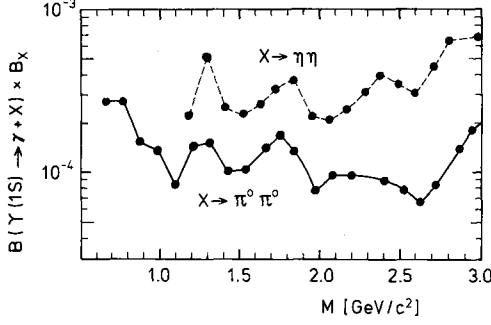


Fig. 3. 90% confidence level upper limits for $B(1S) \times B_X = B(Y(1S) \rightarrow \gamma X) \times B(X \rightarrow \pi^0 \pi^0)$ (solid line) and $B(1S) \times B_X = B(Y(1S) \rightarrow \gamma X) \times B(X \rightarrow \eta \eta)$ (dashed line) for narrow resonances X ($\Gamma_X < 50$ MeV). To guide the eye, the data points were connected with a line

light mesons into all-neutral final states. With the factor $1 + 1.28 \sigma_{\text{rel}}$ we convert the product $\varepsilon_{\text{MC}} \varepsilon_{\text{neut}} N_\gamma$ into its value at 90% CL. We obtain:

$$\begin{aligned} B(Y(1S) \rightarrow \gamma + \eta) &< 3.5 \times 10^{-4} \\ B(Y(1S) \rightarrow \gamma + \eta') &< 1.3 \times 10^{-3} \\ B(Y(1S) \rightarrow \gamma + f_2(1270)) &< 8.1 \times 10^{-4} \\ B(Y(1S) \rightarrow \gamma + f_2(1720), f_2 \rightarrow \eta \eta) &< 4.3 \times 10^{-4}. \end{aligned} \quad (4)$$

In Fig. 3 we show as solid points the upper limit on the product branching ratio for the decay chain $Y(1S) \rightarrow \gamma X$, $X \rightarrow \pi^0 \pi^0$ or $X \rightarrow \eta \eta$. For the upper limit calculation, the total width of X was assumed to be $\Gamma_X < 50$ MeV and a step size of 100 MeV was chosen in the X mass corresponding to about our resolution. For both X decay modes the upper limit is in the region of 1×10^{-4} to 5×10^{-4} .

Special search for $Y(1S) \rightarrow \gamma \eta \rightarrow 3\gamma$

The preceding results have been obtained analyzing the moments of multi-photon energy depositions. If such depositions are due to exactly two photons, the maximum likelihood method PIFIT can be employed to disentangle the two photons creating this shower. Such an approach is especially suited for the decay $Y(1S) \rightarrow \gamma \eta$, $\eta \rightarrow 2\gamma$ where the two decay photons from the η merge to create one single energy cluster; only very asymmetric η decays result in the two photons forming distinct clusters. The log-likelihood difference [10] from PIFIT alone is used to discriminate between showers arising from a single photon and from two photons. Application of this method provides a mass spectrum with significantly less background and thus a more direct approach to search for the $Y(1S) \rightarrow \gamma \eta$ decay.

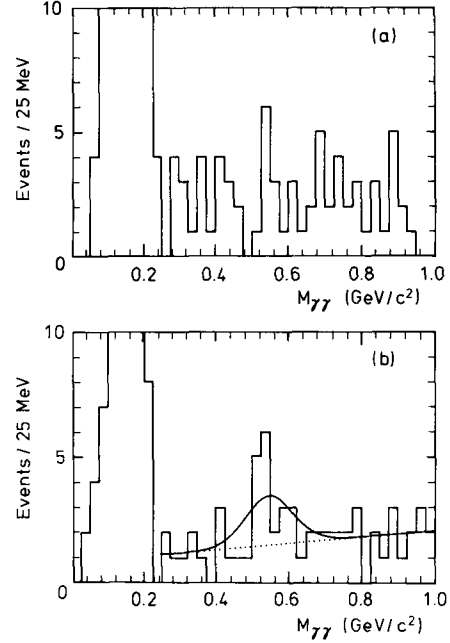


Fig. 4a, b. Invariant mass of energy depositions consistent with originating from two photons. **a** Monte Carlo generated events of the QED process $e^+ e^- \rightarrow \gamma\gamma(\gamma)$, **b** $Y(1S)$ experimental data

We have selected our data for events with two neutral energy clusters well within the fiducial volume of the detector, $|\cos \theta_\gamma| \leq 0.75$, where θ_γ is the angle with respect to the beam direction. The difference of the PIFIT log-likelihoods for the two-photon and one-photon hypotheses was required to be $\Delta\mathcal{L} < 2$ for the photon candidate and larger than 2 for the meson candidate. Furthermore we demand the energy deposition of the photon candidate to be $E_\gamma > 0.80 E_{\text{beam}}$ and of the η candidate to be $E_\eta > 0.65 E_{\text{beam}}$.

Monte Carlo generated events of the QED process $e^+ e^- \rightarrow \gamma\gamma(\gamma)$ indicate that the contribution of this background to a possible η signal is most prominent for the more asymmetric η decays. To remove such events we utilize the fact that the fitting procedure PIFIT also yields the most probable directions and energies of the photons and thus an invariant mass. Monte Carlo studies show that a cut on the lower of the two photon energies $E_\gamma^{\text{low}} < 1.4 M_{\gamma\gamma}$ removes less than 25% of an expected η signal but significantly reduces the QED background. Figure 4a shows after all cuts the invariant mass spectrum from the QED Monte Carlo events corresponding to the same integrated luminosity as the real data. The large peak on the left hand side is due to events from process $e^+ e^- \rightarrow \gamma\gamma$, where PIFIT has converged on a local minimum for the two-photon hypothesis despite a onephoton origin. The cut in $\Delta\mathcal{L}$ forces this peak

to be offset from zero invariant mass. The entries above 200 MeV arise from e^+e^- annihilation into three photons. No enhancement at the position of the η mass is visible.

Figure 4b shows the invariant mass spectrum of the meson candidate for the $\Upsilon(1S)$ data. This spectrum is consistent in shape and magnitude with the QED Monte Carlo spectrum, except for a possible slight enhancement around the η mass. A fit with a Gaussian of fixed width $\sigma = 63$ MeV, determined from Monte Carlo simulation, yields 12.4 ± 5.7 events at $M_{\gamma\gamma} = (548 \pm 28)$ MeV/ c^2 , consistent with the nominal η mass. As the significance is only 2.3 standard deviations, we prefer to calculate an upper limit at 90% confidence level and obtain

$$B(\Upsilon(1S) \rightarrow \gamma + \eta) < 3.9 \times 10^{-4}. \quad (5)$$

This result is in agreement with the upper limit obtained using the global shower technique.

Discussion and summary

The results for $\Upsilon(1S)$ radiative decays to η , η' , $f_2(1270)$ and $f_2(1720)$ are presented in Table 1 together with a result obtained by CLEO [15] and various theoretical predictions. Our results on radiative $\Upsilon(1S)$ decays to η and η' are the only available limits. The CLEO limit on the $f_2(1270)$ is much more stringent than ours, due to the lower background and larger efficiency for the $\pi^+\pi^-$ decay mode, which they use. CLEO has also searched for the $f_2(1720)$ in the channel K^+K^- and obtained a limit on the product branching ratio of 3.2×10^{-5} .

Two different approaches have been used to calculate radiative decay widths of a heavy vector meson to light mesons. Both approaches yield predictions for J/ψ radiative decays which are in good agreement with the measured branching ratios. However, the predictions for $\Upsilon(1S)$ radiative decays differ substantially. Deshpande and Eilam [6], Körner et al. [5] and Tye [7] use the QCD calculation for the photon spectrum in radiative decay to two gluons and scale to the corresponding experimental J/ψ branching ratios. The rather large rates predicted by Deshpande and Eilam [6] were obtained by introducing an ad hoc factor of 3, to account for the deviation between the experimental and theoretical inclusive photon spectrum observed on the J/ψ . Otherwise, the deviations between these predictions reflect the implicit uncertainties in the QCD approach. In contrast to the QCD calculations, Intemann [17] has studied radiative decays within the framework of an extended vector meson dominance model and obtained predictions which are substantially lower than those from the

Table 1. Experimental results (upper limits at 90% confidence level) and theoretical predictions for branching ratios in units of 10^{-5} for radiative decays of the $\Upsilon(1S)$. Also included are the corresponding branching ratios for the J/ψ , which are taken from the Particle Data Group [2] except for the branching ratio to the $f_2(1720)$, which is taken from [16]

$\Upsilon(1S) \rightarrow$	$\gamma + \eta$	$\gamma + \eta'$	$\gamma + f_2(1270)$	$\gamma + f_2(1720)$ $f_2 \rightarrow \eta\eta$
Crystal Ball CLEO [15]	<35	<130	<81 < 4.8	<43
Deshpande, Eilam [6]	15	100		
Körner et al. [5]	3	16	14	~ 1
Tye [7]	2	11	5	~ 1
Intemann [17]	0.06	0.25		
$J/\psi \rightarrow$	$\gamma + \eta$	$\gamma + \eta'$	$\gamma + f_2(1270)$	$\gamma + f_2(1720)$ $f_2 \rightarrow \eta\eta$
From [2, 16]	86 ± 8	420 ± 50	160 ± 20	26 ± 11

QCD inspired methods. The smallness of the branching ratios is primarily due to a dynamical suppression of the $\gamma - Y$ coupling when evaluated off mass shell. All the predictions listed in Table 1 are below our upper limits.

In conclusion, no signal is seen for radiative decays of the $\Upsilon(1S)$ resonance into the light mesons η , η' , $f_2(1270)$ and $f_2(1720)$. Although the present experimental sensitivity is more than sufficient to probe the ranges of the corresponding J/ψ branching ratios (Table 1), the experimental upper limits are not yet stringent enough to test different theoretical models predicting these decays. Also no signal is seen for radiative decays to mesons which decay into $\pi^0\pi^0$ or into $\eta\eta$. The latter channel is of interest for gluonium states in general and the gluonium candidate $f_2(1720)$ in particular. Overall, our measured upper limits are smaller than the branching ratios measured on the J/ψ , indicating a suppression of radiative decays on the $\Upsilon(1S)$ resonance. Due to the coupling of the photon to the quark, a natural suppression factor of $(e_b/e_c)^2 = 1/4$ is expected, which is approximately observed for the leptonic branching ratio. However, our limits are not strong enough to test a further suppression expected to arise from the mass ratio $(m_c/m_b)^2$.

Acknowledgments. We would like to thank the DESY and SLAC directorates for their support. This experiment would not have been possible without the dedication of the DORIS machine group as well as the experimental support groups at DESY. The visiting groups would like to thank the DESY-laboratory for the hospitality extended to us while working at DESY. Z.J., B.N., and G.N. thank DESY for financial support. D.W. acknowledges support from the National Science Foundation. E.D.B., R.H., and K.S. have benefit-

ted from financial support from the Humboldt Foundation. The Nijmegen group acknowledges the support of FOM-ZWO. The Erlangen, Hamburg, and Würzburg groups acknowledge financial support from the German Federal Minister for Research and Technology (BMFT) under the contract numbers 054 ER 11P(5), 054 HH 11P(7), 054 WU 11P(1) and from the Deutsche Forschungsgemeinschaft (Hamburg). This work was supported in part by the U.S. Department of Energy under Contract No. DE-AC03-81ER40050 (CIT), No. DE-AC02-76ER03066 (CMU), No. DE-AC02-76ER03064 (Harvard), No. DE-AC02-76ER03072 (Princeton), No. DE-AC03-76SF00515 (SLAC), No. DE-AC03-76SF00326 (Stanford), and by the National Science Foundation under Grants No. PHY75-22980 (CIT), No. PHY81-07396 (HEPL), No. PHY82-08761 (Princeton).

References

1. T. Appelquist et al.: Phys. Rev. Lett. 34 (1975) 365; S.J. Brodsky et al.: Phys. Lett. 73 B (1978) 203; H. Fritsch, K.H. Streng: Phys. Lett. 74 B (1978) 90; A. Billoire et al.: Phys. Lett. 80 B (1979) 381
2. Particle Data Group, Review of Particle Properties: Phys. Lett. 170 B (1986) 1
3. D.L. Scharre et al.: Phys. Lett. 97 B (1980) 329; C. Edwards et al.: Phys. Rev. Lett. 49 (1982) 259
4. C. Edwards et al.: Phys. Rev. Lett. 48 (1982) 458
5. J.G. Körner, J.H. Kühn, M. Kramer, H. Schneider: Nucl. Phys. B 229 (1983) 115; J.H. Kühn: Phys. Lett. 127 B (1983) 257
6. N.G. Deshpande, G. Eilam: Phys. Rev. D 25 (1982) 270
7. S.H. Tye: Proc. 1982 DPF Summer Study on Elementary Particle Physics and Future Facilities, Snowmass, Colorado, R. Donaldson, R. Gustafson, F. Paige (eds)
8. M. Oreglia et al.: Phys. Rev. D 25 (1982) 2259; E.D. Bloom, C.W. Peck: Ann. Rev. Nucl. Part. Sci. 33 (1983) 143; D. Antreasyan et al.: Phys. Rev. D 36 (1987) 2633
9. R.A. Lee: Ph.D. Thesis Stanford University, SLAC-282 (1985) (unpublished)
10. The difference in the logarithm of the likelihoods is defined as $\Delta\mathcal{L} = \ln \mathcal{L}(1\gamma) - \ln \mathcal{L}(2\gamma)$
11. R.L. Ford, W.R. Nelson: SLAC report SLAC-0210 (1978) (unpublished)
12. For the Monte Carlo generation of all decay chains we used the masses, widths and decay fractions of the produced resonances from the Review of Particle Properties [2]. The $f_2(1720)$ width used in generating Monte Carlo events was taken to be 177 MeV
13. C. Baglin et al.: Nucl. Phys. B 22 (1970) 66
14. M. Cerrada et al.: Nucl. Phys. B 126 (1977) 189
15. A. Bean et al.: Phys. Rev. D 34 (1986) 905
16. K. Königsmann: Phys. Rep. 139 (1986) 243
17. G.W. Intemann: Phys. Rev. D 27 (1983) 2755